

Impact of climate and land use change on the hydrology of a large-scale agricultural catchment

Lieke van Roosmalen,¹ Torben O. Sonnenborg,² and Karsten H. Jensen¹

Received 5 December 2007; revised 21 November 2008; accepted 19 January 2009; published 18 March 2009.

[1] This paper presents a quantitative comparison of plausible climate and land use change impacts on the hydrology of a large-scale agricultural catchment. An integrated, distributed hydrological model was used to simulate changes in the groundwater system and its discharge to rivers and drains for two climate scenarios (2071–2100). Annual groundwater recharge increased significantly (especially the B2 scenario), giving higher groundwater heads and stream discharges and amplifying the seasonal dynamics significantly. Owing to drier summers, irrigation volumes increased by up to 90% compared to current values. Changing the land use from grass to forest had a minor effect on groundwater recharge, whereas CO₂ effects on transpiration resulted in a relatively large increase in recharge. This study has shown that climate change has the most substantial effect on the hydrology in this catchment, whereas other factors such as irrigation, CO₂ effects on transpiration, and land use changes affect the water balance to a lesser extent.

Citation: van Roosmalen, L., T. O. Sonnenborg, and K. H. Jensen (2009), Impact of climate and land use change on the hydrology of a large-scale agricultural catchment, *Water Resour. Res.*, 45, W00A15, doi:10.1029/2007WR006760.

1. Introduction

[2] The most recent Intergovernmental Panel on Climate Change (IPCC) report states that global atmospheric concentrations of greenhouse gases (GHG) have increased markedly since 1750 as a result of human activities [Intergovernmental Panel on Climate Change (IPCC), 2007]. IPCC predicts that GHG concentrations will continue to rise during the present century at rates determined by global economic development with significant impacts on the future climate. The increase in carbon dioxide concentrations is mainly caused by the burning of fossil fuels, but the contribution of land use changes (primarily deforestation) is also significant [IPCC, 2007]. From a hydrological perspective, another relevant aspect of land use change in a changing climate is its role in propagating changes in meteorological variables, such as precipitation and evapotranspiration to the surface and groundwater system. The vegetation type determines the transpiration properties through the crop factor and the root depth, and the fraction of precipitation that is intercepted by the canopy. Land use changes can therefore reduce or amplify future climate change induced hydrological impacts in a catchment.

[3] A number of studies have focused on the effects of climate change on hydrological systems in Europe [e.g., Andréasson *et al.*, 2004; Arnell, 1999; Caballero *et al.*, 2007; Graham *et al.*, 2007b; Kleinn *et al.*, 2005; Thodsen, 2007]. Generally, the simulated impacts of climate change vary considerably as a result of contrasting climate change

signals in northern and southern Europe, e.g., an increase in annual precipitation in the north and a decrease in the south and much larger increases in summer temperatures in southern Europe than in northern Europe [Christensen and Christensen, 2007]. Also, more regional characteristics, such as orography and distance to the coast, affect how the large-scale changes in climate emerge locally. For example, Andréasson *et al.* [2004] found that the largest increases in runoff occurred in the mountainous northwestern parts of Sweden, whereas southeastern Sweden showed decreasing runoff as a result of considerably drier conditions. Not only climate change causes large variations in the simulated impacts, but also differences in the dominant hydrological processes under present conditions are important. An increase in extreme summer precipitation events [Christensen and Christensen, 2004] can have a considerable impact in an area where surface runoff is the dominant process, but have a smaller impact on groundwater-fed systems. Owing to the heterogeneity of the meteorological conditions and the heterogeneous physiographical conditions, climate and land use change impact studies on hydrology often have a local to regional character.

[4] The majority of hydrological climate change impact studies focus on surface water, i.e., rainfall-runoff processes [e.g., Christensen *et al.*, 2004; Graham *et al.*, 2007a; Vanrheenen *et al.*, 2004], whereas Allen *et al.* [2004] pointed out that fewer studies investigate the impact of climate change on groundwater [Allen *et al.*, 2004; Bouraoui *et al.*, 1999; Brouyère *et al.*, 2004; Jyrkama and Sykes, 2007; Loáiciga *et al.*, 2000; Scibek and Allen, 2006a, 2006b; Scibek *et al.*, 2007; Varanou *et al.*, 2002; Woldeamlak *et al.*, 2007]. While climate change affects surface water directly through changes in the major long-term climate variables, the relationship between the changing climate and groundwater is more complicated because of the direct interaction

¹Department of Geography and Geology, University of Copenhagen, Copenhagen, Denmark.

²Geological Survey of Denmark and Greenland, Copenhagen, Denmark.

with surface water resources and the indirect influence of the recharge process [Jyrkama and Sykes, 2007]. Available studies show that groundwater recharge is a function of the changes in the meteorological input based on the selected climate scenario in combination with landscape characteristics, e.g., soil types, land use, and depth to the water table and human impacts such as drainage, groundwater abstractions, and flow regulation. Jyrkama and Sykes [2007] showed that groundwater recharge in the Grand River watershed, Ontario, increased owing to climate change and that spatially the changes in recharge varied considerably, depending on the variations in land use and soil types. Scibek and Allen [2006a] compared the potential impacts of climate change on two unconfined aquifers in western Canada and the United States; one dominated by recharge and the other dominated by river-aquifer interaction. The changes in groundwater levels of the two geologically similar aquifers differed substantially owing to the differences in predicted climate change and in the degree of interaction with surface water.

[5] Woldeamlak *et al.* [2007] analyzed the sensitivity to climate change of water balance components for a sandy aquifer under temperate conditions in Belgium using an uncoupled water balance module to compute recharge and a steady state groundwater model (MODFLOW). The climate scenario simulations showed increases in surface runoff, groundwater recharge, and evapotranspiration for all seasons and annual totals, except for the summer groundwater recharge. The larger increases in winter precipitation relative to summer precipitation resulted in an increase in the proportion of annual groundwater recharge occurring during winter from 86% in the present climate to 98% in the year 2100. High evapotranspiration during summer was mainly attributed to forests because forests were able to utilize most of the increase in soil moisture storage that came from winter recharge. For future studies Woldeamlak *et al.* [2007] suggested use of transient models to study seasonal variations of the groundwater components, inclusion of land use change scenarios, and an improved representation of the coupling between groundwater and surface water.

[6] Only a limited number of these studies focusing on groundwater and climate change included the use of an integrated hydrological model. The advantage of using an integrated groundwater-surface water model is that it enables studying certain feedback processes, such as a possible increase in actual evapotranspiration as a result of higher groundwater levels or a decrease in river discharge due to afforestation. An integrated, process-based hydrological model is the most appropriate tool to investigate the intricate, nonlinear relationships between the land surface, the unsaturated zone, and the saturated zone under changing conditions, though the large number of parameters complicates using such models.

[7] At present, very few studies have quantified the combined effects of future climate and land use changes on hydrology [Quilbe *et al.*, 2008]. Pfister *et al.* [2004] studied changes in peak flows in the Rhine and Meuse basins due to climate and land use change from a historic perspective to gain a better understanding of the dominating processes in the catchment and also simulated future changes in climate and land use. Generally, the results showed a very limited effect of future land use change in

comparison with the impact of climatic change. Notter *et al.* [2007] investigated climate and land use change in an area climatologically very different from Denmark, namely the Mt. Kenya area. Conversion of the forest area to crop or grass land increased annual runoff by 11% and 59%, respectively, while climate change impacts resulted in an increase in annual runoff of 26%. Loukas *et al.* [2002] included altitudinal shifts in vegetation due to higher temperatures, changes in tree cover, density, and plant physiology in the simulations of future climate change for two catchments in British Columbia, Canada. Average annual actual evapotranspiration decreased by 19% and 22% for the two catchments, showing that the increased biomass of the vegetation only partly compensated for the 30% reduction in transpiration due to stomatal closure, as a result of the higher atmospheric CO₂ concentration.

[8] The aim of this study is to determine the sensitivity of the hydrological system to a number of meteorological and land use factors, which are expected to change in a future climate. A large-scale agricultural catchment with a groundwater-based hydrological system in Denmark was selected for the analysis. An integrated, distributed, physically based model called the DK model [Henriksen *et al.*, 2003; Sonnenborg *et al.*, 2003] was used to study changes in the groundwater system and its discharge to rivers and drains. The climate change impacts were simulated using climate-forcing data for the SRES A2 and B2 scenarios [IPCC, 2000] for the period 2071–2100 and by raising the sea level to +0.5 m above sea level (masl) and +1 masl. The land use change effects include impacts on irrigation demand, doubling the area with forest at the expense of grain and grass, changes in crop development dates, and a reduction in crop transpiration in the scenario climate simulations. Hydrological model output, such as water balance components, groundwater heads, stream discharges, and irrigation volumes are compared for a 15-year period. The novelty of this study is a quantitative comparison of climate change effects and water management impacts on a groundwater system using a spatially distributed and integrated groundwater-surface water model, which makes it possible to include feedback processes of the simulated changes.

2. Study Area

[9] The study area is located in the western part of Jutland, Denmark, between the Jutland Ridge and the west coast (Figure 1) with an area of 5459 km². The topography slopes gently from east to west with land surface elevations from 125 masl in the eastern part to sea level at the coast. Land use is defined as grain and corn (56%), grass (29%), forest (7%), heather (5%), and urban (2%) on the basis of satellite data. Most of the forest consists of conifer trees. Since 1990 the agricultural area covered by corn has increased from less than 1% to approximately 10% at the expense of root crops (primarily beets) and rape [Statistics Denmark]. However, in this study grain and corn are pooled together and represented by grain (see Figure 1). The area is bounded by the North Sea to the west, while the Jutland Ridge serves as the boundary to the east. The northern and southern boundaries are delineated on the basis of local water divides.

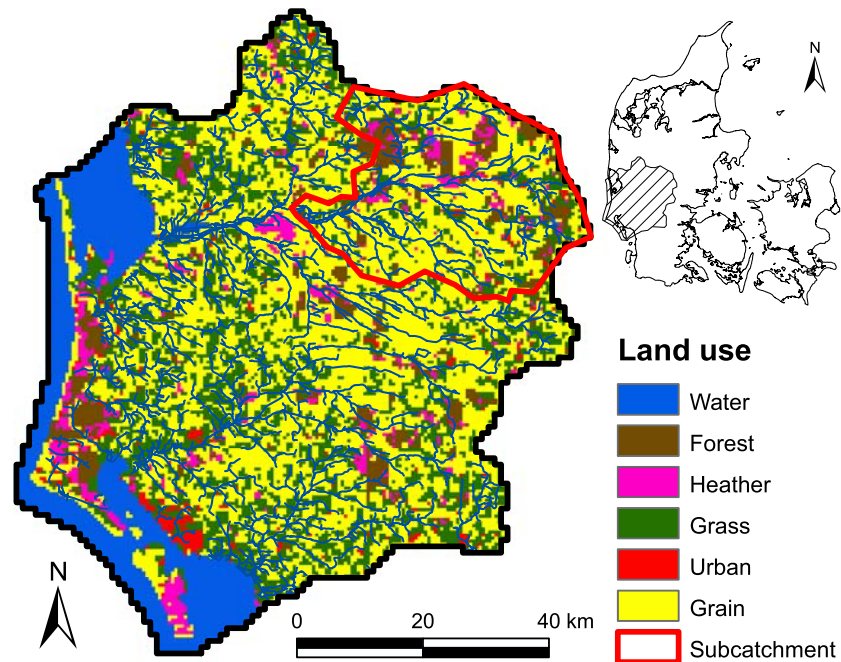


Figure 1. Map showing the land use in the catchment. The subcatchment (indicated in red) is used to study the effects of land use changes. The inset shows the location of the study area in Denmark.

2.1. Climate and Hydrology

[10] The climate in western Jutland is typical of the maritime regime, dominated by westerly winds and frequent passages of extratropical cyclones. Maximum precipitation is in autumn and minimum in spring. The dominant westerly wind results in mild winters and relatively cold summers with highly variable weather conditions characterized by frequent rain and showers.

[11] The Danish Meteorological Institute has developed a climate grid for Denmark [Scharling, 1999] providing daily values for temperature, precipitation, and reference evapotranspiration ET_{ref} (potential evapotranspiration for a well watered grass of uniform height) at a 40-km resolution. For each grid cell representative time series are estimated on the basis of data from available climate stations. For this study we have retrieved data for the period 1990–2004. The precipitation is corrected for wetting and aerodynamic effects using the standard correction methods of *Allerup et al.* [1998]. The average precipitation in the area equals 1073 mm/a. ET_{ref} is calculated using the *Makkink* [1957] formula, and has an average value of 570 mm/a. The average annual temperature is 8.2°C with a maximum of 16.5°C in August and a minimum of 1.4°C in January.

[12] The central and northern part of the area is drained by the Skjern River system, while the southern part is drained by the two smaller stream systems Varde Stream and Sneum Stream (Figure 2). The river discharge out of the area amounts to approximately 470 mm/a [Ovesen et al., 2000]. Owing to the highly permeable soils all water outside the wetlands infiltrates, and the discharge to the streams is dominated by groundwater base flow.

2.2. Geology and Hydrogeology

[13] The main ice border of the Weichselian glaciation was located at the Jutland Ridge, hence the shallow geology in Western Jutland is dominated by glacial outwash sand

and gravel originating from the glaciers' meltdown. Isolated islands of Saalian sandy till are found between the outwash plains (Figure 2). The thickness of the Quaternary deposits is generally less than 50 m in the central and northeastern

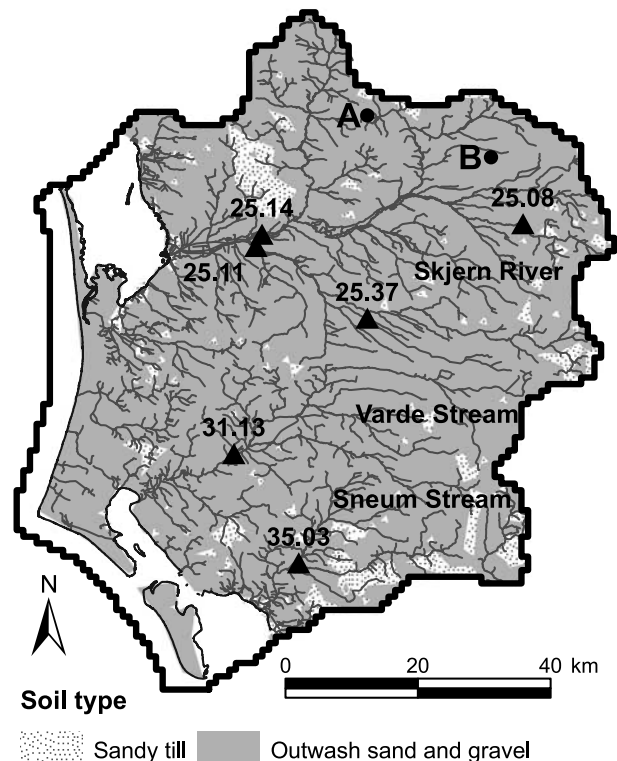


Figure 2. Map showing the soil types in the catchment. Six discharge stations (triangles) are indicated. Locations A and B indicate the wells for which the time series are shown in Figure 5.

part of the area, while the thickness increases in the southern and western part and in some places reaches depths of approximately 250 m. Miocene sediments are found below the Quaternary deposits. The Miocene sediments are formed by alternating layers of clayey and sandy marine deposits with a total thickness of generally 200–300 m. The Miocene layers dip slightly to the west. Beneath the Miocene sequence, Paleogene clay sediments of regional extent are found. The Paleogene unit is conceptualized as an aquitard that acts as a lower boundary to groundwater flow.

[14] The Quaternary and Miocene sand formations often form large interconnected aquifers. The hydraulic conductivity of the sand formations is generally high, of the order of 10^{-4} – 10^{-3} m/s [Harrar *et al.*, 2003; Sonnenborg *et al.*, 2003]. In general, groundwater flows from east to west. At the water divide to the east the hydraulic head level is about 75 masl, decreasing to sea level at the west coast. The average head gradient is 0.001. The seasonal variation in head values is generally less than 1 m.

[15] Groundwater abstraction varies seasonally as well as yearly owing to variable demands for irrigation. Abstraction for domestic and industrial purposes amounts to approximately 10 mm/a. A model study for the area showed an average groundwater abstraction for irrigation of approximately 20 mm/a [Henriksen and Sonnenborg, 2003]. However, the demand for irrigation can be up to 50 mm/a in dry summers, which is the maximum amount licensed by the local government. 80% of the water is abstracted from aquifers located above –20 masl [Henriksen and Sonnenborg, 2003].

3. Methods

3.1. Climate-Forcing Data

[16] The confidence in Atmosphere–Ocean general circulation models (GCM) providing credible quantitative estimates of future climate change has increased the past few years [Meehl *et al.*, 2007]. However, these simulations are particularly useful at large scales, making it necessary to downscale the outputs for use in regional, hydrological models. In this study, a physically based, regional climate model (RCM) HIRHAM, developed by the Danish Meteorological Institute [Christensen *et al.*, 1996, 1998] is used to dynamically downscale the climate change signals projected by the general circulation model HadAM3H developed by the Hadley Centre. The RCM is driven by sea surface temperatures and atmospheric lateral boundary values from the forcing GCM [Déqué *et al.*, 2005]. Output is extracted for the IPCC A2 and B2 scenarios [IPCC, 2000].

[17] The choice of forcing GCM can have considerable effect on the projected future changes by the RCM [Déqué *et al.*, 2007]. Christensen and Christensen [2007] compared a suite of RCM simulations, which among others included two RCMs which were forced each by two different GCMs, namely HadAM3H and ECHAM4/OPYC3 for the A2 scenario. Generally, the RCM simulations with ECHAM4/OPYC3 showed a much stronger warming than simulations with HadAM3H. For example, the increase in temperature for HIRHAM forced by ECHAM4/OPYC3 was 1.0° higher for Scandinavia and 1.3° higher for Middle Europe than when forced by HadAM3H. Denmark is located on the border between these two study areas. Only marginal differ-

ences were found in the changes in winter precipitation when going from HadAM3H to the RCMs because changes in winter precipitation in the RCMs followed, to a large degree, the changes in the general atmospheric circulation. The ECHAM-driven experiments showed similar precipitation change patterns as the HadAM3H-driven experiments except that the increases in winter and spring precipitation in northern Scandinavia were much larger. For Scandinavia winter precipitation increased with 35% for the HIRHAM experiments driven with ECHAM compared with a 23% increase for HIRHAM–HadAM3H. In summer, precipitation decreased with 20% and 2% for the HIRHAM experiments using HadAM3H and with 30% and 7% for the ECHAM-driven experiments for Middle Europe and Scandinavia, respectively.

[18] RCM output is not available for the entire period 1961–2100 because transient RCM simulations are computationally very demanding. Instead two 30-year time slices are available; one representative for the climate in the period 1961–1990 (control) and the other representing future climate in 2071–2100 (scenario). It is very uncertain how society will adapt to climate change, thus it should be noted that the A2 and B2 scenarios used in this study are only two plausible descriptions of how future GHG emissions might develop and these scenarios are not any more likely than any other scenario. The developments described for the second half of the 21st century are even more uncertain than for the first part of the century, owing to the longer time span. The main reasons for choosing a period (2071–2100) so far in the future are (1) the change signals from the scenarios are generally weaker for the first half of the century, and it is therefore difficult to distinguish a clear climate change signal for earlier periods owing to natural variability and (2) the change signals from the individual scenarios are difficult to distinguish from each other before the end of the century.

[19] Because of systematic biases between the RCM simulation of the historic climate (1961–1990) and the observed climate, a transfer method is necessary to construct the climate scenario data sets for the hydrological model simulations. Here the delta change method [Hay *et al.*, 2000] is applied, which consists of perturbing baseline meteorological data with monthly change values. The monthly change values are calculated from the differences in atmospheric outputs from the RCM for the current climate (1961–1990) and the scenario period (2071–2100). The meteorological input used as a baseline for the climate-forcing data sets for the scenario simulations are the observed daily precipitation, temperature, and ET_{ref} data of the climate grid for Denmark. The same input data are used for the hydrological simulations of the current climate.

[20] The correction method for precipitation can be formulated as

$$P_{\Delta}(i,j) = \Delta_P(j) \times P_{obs}(i,j); \quad i = 1, 2, \dots, 31; \quad j = 1, 2, \dots, 12 \quad (1)$$

where P_{Δ} is the precipitation input to the hydrological model for the A2 and B2 scenario runs and P_{obs} is the observed precipitation representing the current climate. The suffixes i and j stand for the i th day of the j th month. Δ_P is

the delta change value, which is calculated using the expression

$$\Delta_P(j) = \frac{\bar{P}_{scen}(j)}{\bar{P}_{cont}(j)}; \quad j = 1, 2, \dots, 12 \quad (2)$$

where $\bar{P}(j)$ is the precipitation in month j averaged for the 30-year control or scenario period as simulated by the RCM. The index *scen* stands for the scenario period (2071–2100) and the index *cont* indicates the control period (1961–1990). For ET_{ref} the delta change values are calculated in a similar manner. ET_{ref} is not direct output from the RCM but is calculated using the FAO Penman-Monteith equation [Allen *et al.*, 1998] and RCM output such as incoming and outgoing, short- and long-wave radiation, temperature, water vapor pressure, and wind speed:

$$ET_{ref} = \frac{0.408\Delta(R_n - G) + \gamma \frac{900}{T + 273} u_2 (e_s - e_a)}{\Delta + \gamma(1 + 0.34u_2)} \quad (3)$$

where ET_{ref} is reference evapotranspiration (mm d^{-1}), R_n is net radiation at the crop surface ($\text{MJ m}^{-2} \text{d}^{-1}$), G is soil heat flux density ($\text{MJ m}^{-2} \text{d}^{-1}$), T is mean daily air temperature at 2 m height ($^{\circ}\text{C}$), u_2 is wind speed at 2 m height (m s^{-1}), $e_s - e_a$ is saturation vapor pressure deficit (kPa), Δ is the slope of the vapor pressure curve ($\text{kPa } ^{\circ}\text{C}^{-1}$), and γ is the psychrometric constant ($\text{kPa } ^{\circ}\text{C}^{-1}$).

[21] ET_{ref} as described in equation (3) is the potential evapotranspiration for a hypothetical grass reference crop with an assumed crop height of 0.12 m, a fixed surface resistance of 70 s m^{-1} , and an albedo of 0.23 [Allen *et al.*, 1998].

[22] For temperature the absolute change is used for the delta values

$$T_{\Delta}(i, j) = T_{obs}(i, j) + \Delta_T(j) \quad (4)$$

where Δ_T is given by

$$\Delta_T(j) = \bar{T}_{scen}(j) - \bar{T}_{cont}(j); \quad j = 1, 2, \dots, 12 \quad (5)$$

A more detailed description of the construction of the data sets can be found by van Roosmalen *et al.* [2007].

[23] HIRHAM output for the A2 scenario is available at a horizontal grid resolution of 12 km and the B2 scenario at a 50 km resolution. The B2 scenario is a more moderate scenario than the A2 scenario, resulting in lower temperature increases. The mean annual temperature in the catchment increases 2.2°C for the B2 scenario and 3.2°C for the A2 scenario. The increases in mean annual precipitation are 116 mm (12%) and 160 mm (16%) for the A2 and B2 scenarios, respectively. The increase in annual ET_{ref} is 110 mm (19%) for the A2 scenario and 80 mm (14%) for the B2 scenario. Figure 3 shows mean monthly temperature, precipitation, and ET_{ref} for the current climate and both climate scenarios.

3.2. Hydrological Model

[24] The hydrological model used in this study is based on the National Water Resources Model for all of Denmark (the DK model), described by Henriksen *et al.* [2003] and Sonnenborg *et al.* [2003]. The DK model is a distributed and integrated groundwater-surface water model based on

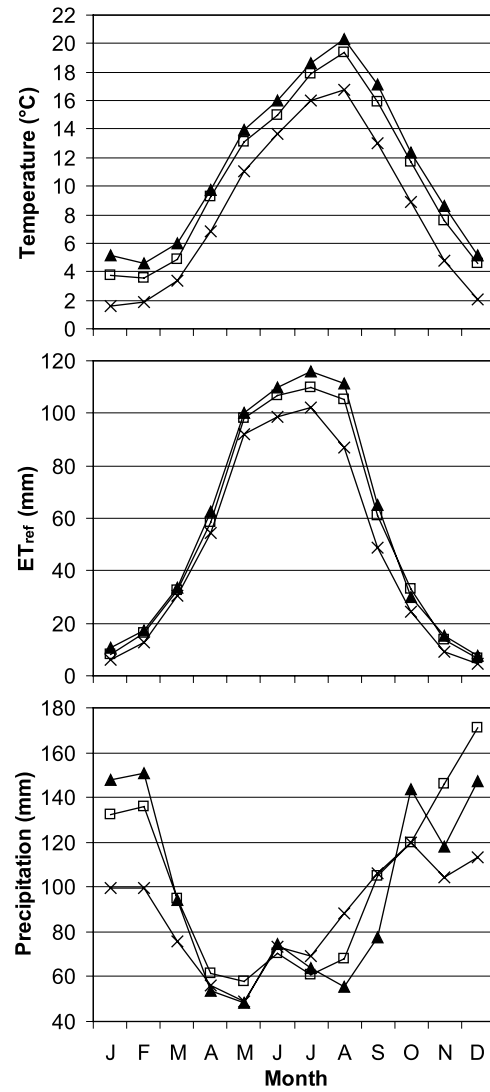


Figure 3. Mean monthly temperature ($^{\circ}\text{C}$), precipitation (mm), and reference evapotranspiration (mm) for the current climate (crosses) and the A2 (triangles) and B2 (squares) scenarios.

the MIKE SHE code [Refsgaard and Storm, 1995; Graham and Butts, 2006]. Using detailed information on the geology and associated hydraulic parameters, 3-D groundwater flow is solved on the basis of Darcy's law. Much attention has been paid to the description of the geological settings in the model, such that groundwater flow can be described at high spatial resolution (horizontal discretization is 500 m and vertically 16 model layers are used). The DK model was developed for water resources assessment and planning and as 99% of the water supply in Denmark is based on groundwater, it is important that this model accurately describes the groundwater processes. Groundwater also constitutes a large part of the flows in streams, particularly during low flow. The DK model has documented predictive capabilities at a regional and catchment scale [Henriksen *et al.*, 2003], making it a suitable tool for scenario-based hydrological impact studies.

[25] Interaction between groundwater and rivers is described as either base flow or drain flow. Base flow is

Table 1. Two-Layer Unsaturated Zone Parameters^a

	θ_{sat}	θ_{fc}	θ_{wp}	Z_{surf} (mbgs)
Sand	0.3	0.15	0.03	0.35
Sandy till	0.4	0.25	0.06	0.50

^a θ , average moisture content; sat, saturated conditions; fc, field capacity; wp, wilting point; Z_{surf} , the lowest elevation of the water table in meters below ground surface (mbgs) where the capillary zone still reaches the ground surface.

modeled using a Darcy type relationship between flux and head difference, where a base flow leakage coefficient, that depends on the river bottom permeability, acts as the controlling parameter. Drain flow is modeled as a linear reservoir where drain flow is generated if the groundwater table is located above the specified drainage level. The drain system captures flow through small streams, ditches and drain pipes that cannot explicitly be described in a large-scale model. The drain flow is calculated on the basis of distributed information on drain levels and drainage coefficients, and is routed to the nearest river or the sea. River flow is simulated on the basis of river geometry, slope, and the Manning roughness factor using the Muskingum-Cunge routing method [Chow *et al.*, 1988] as implemented in the MIKE 11 model [Havne *et al.*, 1995].

[26] The original model is modified in several ways to make it more suitable for this study. For example, topographic data at a 500×500 m horizontal resolution are included and the horizontal discretization is changed from 1×1 km to 500×500 m to better describe the land surface variations and improve representations of streams. The unsaturated zone is included as an integrated part of the model, with the purpose to (1) simulate the interaction between changes in groundwater level and evapotranspiration and (2) simulate irrigation water demand for the future climate as a function of water content in the root zone. A more detailed land use classification was introduced on the basis of a satellite image for 9 May 2001, making it possible to study the effects of land use change.

3.3. Model Setup

[27] The model described above is used in transient mode for the period 1971–2004 of which 1971–1989 is a spin-up period, where the model is allowed to adjust itself to the prevailing hydrological conditions, while the period 1990–2004 is used as the period for the hydrological interpretations.

3.3.1. Unsaturated Zone

[28] Unsaturated zone processes are computed by a two-layer water balance method [Yan and Smith, 1994] available in the MIKE SHE system [DHI, 2007]. The two-layer method is a relatively simple water balance method for calculating actual evapotranspiration and groundwater recharge. The controlling parameter is the root zone capacity, defined as the difference between water content at field capacity and wilting point, multiplied by the depth of the root zone. The higher the root zone capacity, the higher the fraction of infiltrating water that can be removed by evapotranspiration is. For the two-layer unsaturated zone module the parameters presented in Table 1 are used.

3.3.2. Irrigation

[29] Irrigation is described using a “shallow well source” implemented in MIKE SHE, whereby water is extracted from the same location as where it is used. A maximum

depth to the water table is specified, and pumping will stop, if the water level drops below that depth. The irrigation water is applied as sprinkler irrigation, which is the typical irrigation method in Western Jutland, and using this method the irrigation water is simply added to the precipitation component. Irrigation is applied to the area covered by grain and grass (see Figure 1).

[30] Irrigation is specified to start when the soil water deficit SWD exceeds the threshold value SWD_{ir} . SWD is defined by

$$\text{SWD} = \frac{\theta_{\text{fc}} - \theta_{\text{act}}}{\theta_{\text{fc}} - \theta_{\text{wp}}} \quad (6)$$

where θ_{fc} is the water content at field capacity, θ_{act} is the actual water content, and θ_{wp} is the water content at wilting point. Irrigation is applied until the actual water content equals the water content at field capacity. The threshold value for soil water deficit is specified as $\text{SWD}_{\text{ir}} = 50\%$, resulting in irrigation when the available water content is less than 50% of the maximum available water content in the root zone.

3.3.3. Saturated Zone

[31] In the vertical plane the model is resolved using 16 model layers. To avoid overparameterisation of the model, uniform parameter values are used for the five geological units defined in the hydrostratigraphical model. These units are Quaternary clay, Quaternary sand, Quartz sand, Mica sand, and Mica clay/silt. Automatic parameter estimation using UCODE [Poeter and Hill, 1998] yielded the corresponding horizontal conductivity values: 6.2×10^{-8} m/s, 2.2×10^{-4} m/s, 2.8×10^{-4} m/s, 9.8×10^{-5} m/s, and 1.6×10^{-6} m/s. The coefficient for drain flow is specified as $2 \times 10^{-7} \text{ s}^{-1}$ and the base flow leakage coefficient as $2.7 \times 10^{-6} \text{ s}^{-1}$.

3.3.4. Land Use

[32] Parameterizations of the land use types are provided in Table 2. The parameters for grain vary throughout the 136 days of the growing season, which starts on 1 April and ends 15 August each year. The growing season is divided into four stages, with maximum values of the leaf area index (LAI) and root depth (d_r) from day 60 until harvest. From day 60 the crop factor K_c for grain equals 1.05 and then increases to a maximum of 1.15 on day 75, after which K_c reduces to 1.05 at harvest time. After the growing season the grain area is assumed to be represented by bare soil for the winter season.

[33] The other land use types have constant parameters throughout the year, except for LAI values for grass, which increase from 2.2 on 1 April to 4.5 in approximately 60 days, when the grass is cut and the LAI value is set to 2.2 again. Grass is cut three times during the growing season from April to the beginning of September. The K_c value used for forest is relatively high. However, on the basis of investigations by Mossin and Ladekarl [2004] and van der Salm *et al.* [2006] evaporation from the intercepted water is responsible for a relatively high potential evapotranspiration from conifer trees in this area.

3.3.5. Sea Level Rise

[34] Two scenarios for the effects of sea level rise, namely a 0.5 m and 1 m increase, are investigated in this study, owing to the uncertain projections related to the future

Table 2. Leaf Area Index, Root Depth d_r , and Crop Factor K_c for the Various Land Use Types^a

	LAI	d_r (m)	K_c
Grain	2.0 – 5.0	0.1 – 1.0	1.0 – 1.15
Bare soil	1.0	0.1	1.0
Grass	2.2 – 4.5	0.5	1.0
Forest	6.0	1.0	1.2
Heather	2.0	0.4	1.0
Urban	1.0	0.1	1.0

^aLAI, Leaf Area Index. LAI and K_c are dimensionless.

climate. The set up for these simulations includes the transformation of all land areas below either 0.5 m or 1 m in the study catchment to sea, the removal of the drains in these areas, and the head boundary condition at the downstream end of the streams is raised from 0 to either 0.5 m or 1 m. From 1870 to 2005, global average sea level rose by nearly 0.2 m [Bindoff *et al.*, 2007] and toward the end of this century, projected sea level rise ranges from 0.23 to 0.51 m for the A2 scenario [Meehl *et al.*, 2007]. The rate of sea level rise from 1993 to 2003 was estimated to be 3.1 ± 0.7 mm/a, which is significantly higher than the average rate of 1.7 ± 0.5 mm/a for the 20th century, but it is unknown whether the higher rate is due to decadal variability or an increase in the long-term trend [Bindoff *et al.*, 2007]. The 1 m sea level rise used in the model set up is considerably higher than the projections, but 1 m is used as an upper bound because of considerable regional variability in sea level change (± 0.15 m for a typical AOGCM model projection) and great uncertainty related to increase in discharge from ice sheets [Lenton *et al.*, 2008].

[35] The eustatic sea level rise could be counterbalanced by the isostatic uplift, which has been occurring in Denmark since the melting of the ice caps. In the work by Mertz [1924] a map shows that the largest uplift occurs in the northernmost part of Denmark, whereas negligible uplift occurs in the middle of Jutland. For our study area no significant influence of isostatic uplifting on the relative sea level is expected as it is located just south of the 0 m uplift line.

3.4. Calibration and Validation

[36] The calibration and validation of the groundwater and river system were performed on the original model and these results are presented here. A more elaborate description is given by van Roosmalen *et al.* [2007]. The changes introduced to the model in this study are not meant to improve the ability of the model to reproduce groundwater head and stream discharge, but to make the model more useful for the analysis presented in this study. The approach is therefore to generate similar results for recharge and stream discharge as the original model. The parameters were calibrated and validated by comparing the simulated annual and monthly recharge to the corresponding results of the original model and by comparing discharges. Recharge is the most important characteristic of the water balance in this system and must therefore be affected as little as possible by the changes in the representation of the surface.

[37] The calibration period for the model was 1991–1995, while the validation period was 1996–1999. The performance of the model was tested against observations of stream discharge and groundwater heads using the root

mean squared error RMS for groundwater head and the RMS and the Nash-Sutcliffe efficiency coefficient E for stream discharge. E is given by [Nash and Sutcliffe, 1970]

$$E = 1 - \frac{\sum_{i=1}^N (Q_{obs,i} - Q_{sim,i})^2}{\sum_{i=1}^N (Q_{obs,i} - \overline{Q_{sim}})^2} \quad (7)$$

where $Q_{obs,i}$ and $Q_{sim,i}$ are the observed and simulated daily discharges, respectively, N is the number of observations, and $\overline{Q_{sim}}$ is the average simulated discharge. A perfect match between simulated and observed values results in an E value of 1. If the simulated values represent the observations worse than the mean of the observed values a negative E value is obtained. RMS is given by [Anderson and Woessner, 1992]

$$RMS = \sqrt{\frac{1}{N} \sum_{i=1}^N (H_{obs,i} - H_{sim,i})^2} \quad (8)$$

where $H_{obs,i}$ and $H_{sim,i}$ are the observed and simulated hydraulic heads, respectively. Similarly for stream discharge, the RMS values are calculated as in equation (8). An RMS value of 0 implies a perfect match between simulated and observed values. The RMS value increases with the discrepancy between the simulated and observed values.

[38] At the downstream discharge stations of the three stream systems an average value of $E = 0.81$ and $RMS = 1.84 \text{ m}^3/\text{s}$ was found for the validation period 1996–1999. Comparison with 4920 groundwater head measurements for the validation period yielded an RMS value of 3.79 m. The validation values are considered excellent for a large-scale hydrological model. The RMS values for the groundwater heads should be compared to the uncertainty of the observed head data. Henriksen and Sonnenborg [2005] estimated the aggregated uncertainty of the observed head data relative to model simulations at a 1 km scale to have a value of 3.1 m, corresponding to RMS values of 6.2 m at the 95% confidence levels. This aggregated uncertainty includes factors such as measurement errors, errors in assessing the elevation of the well, scaling errors due to the 1 km model grid size, and errors due to geological heterogeneity not described by the model.

[39] Figure 4 shows a comparison of observed and simulated discharges for the period 1996–2004 and 1996–1999 for discharge stations 31.13 and 25.14 located in the largest streams in the watershed (Figure 2). As an example of the capability of the model to simulate groundwater heads, Figure 5 presents observed and simulated groundwater heads for the period 1990–2000 at two locations in the watershed (locations A and B in Figure 2). The well screen is located 5.65 m below ground surface at location A and 25.5 m below ground surface at location B. Generally the model captures the dynamics in the time series well, even though the mean simulated and observed values may differ considerably. Therefore this study focuses on spatially averaged changes when comparing one simulation to the other and less on the absolute values at a point.

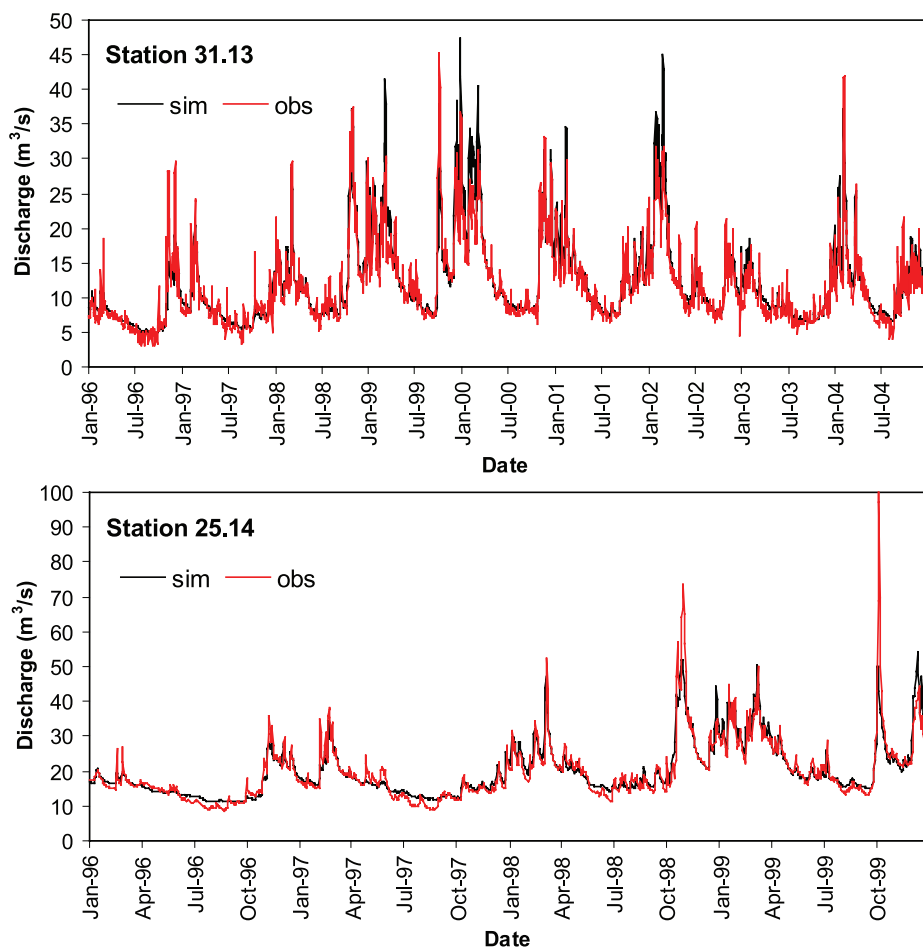


Figure 4. Observed and simulated discharges for the two largest streams in the catchment at discharge stations 31.13 (1996–2004) and 25.14 (1996–1999).

3.5. Analysis of the Sensitivity of Future Climate Changes

[40] The described hydrological model is used to examine plausible future changes in the hydrological system caused by changes in meteorological variables due to increased GHG emissions and changes in sea level, irrigation water demand, and land use and transpiration response to increased CO_2 concentrations. The effect of the individual changes is analyzed and the relative effects are compared. The results of this study are expressed as changes in the scenario simulations compared to the current climate. First, this approach is used because it is not possible to validate the model for scenario simulations. Second, the change in simulated heads or discharge is more significant than the absolute values because the model simulations are highly correlated, making the uncertainty of the changes much smaller than the uncertainty of the absolute values. However, it is very difficult to quantify the uncertainty in the simulated changes. In the discussion in this paper we elaborate on the uncertainties related to the climate scenarios and data, the data transfer method, and the hydrological model structure, while here we focus on the uncertainty related to the parameters of the hydrological model.

[41] A local sensitivity analysis is performed to determine the sensitivity of the simulated heads and discharges to

changes in parameter values. Two times the standard deviation is successively added to the K_h values of the five geological units and the vertical hydraulic conductivities K_v are changed in the same manner assuming $K_v = 0.1 \times K_h$. The values for the drainage and base flow leakage coefficients are also increased by two times the standard deviation. The simulated groundwater heads are compared at 18 locations equally distributed in the catchment and at two depths represented by the numerical layers 1 and 5. Layer 1 is the upper, unconfined aquifer and layer 5 is the deeper main aquifer in the area. Simulated discharge values are compared at six stations (Figure 2). The absolute difference between the simulated heads for the simulation with altered parameters and the original parameter values is calculated at each location and then the mean is calculated for all analysis points in layer 1 and 5. The absolute values of the differences for discharge are also calculated. The sensitivity of the simulated heads to changes in the parameter values is of the order of centimeters with the biggest difference of 0.09 m found for layer 5 when changing K_h for glacial outwash sand. Changes in stream discharges due to changes in the parameters are very small, namely $0.01 \text{ m}^3/\text{s}$, indicating that even small changes in discharge due to climate or land use change are significant. The sensitivity of the groundwater heads and discharges to changes in parameters are very similar for both the current climate and

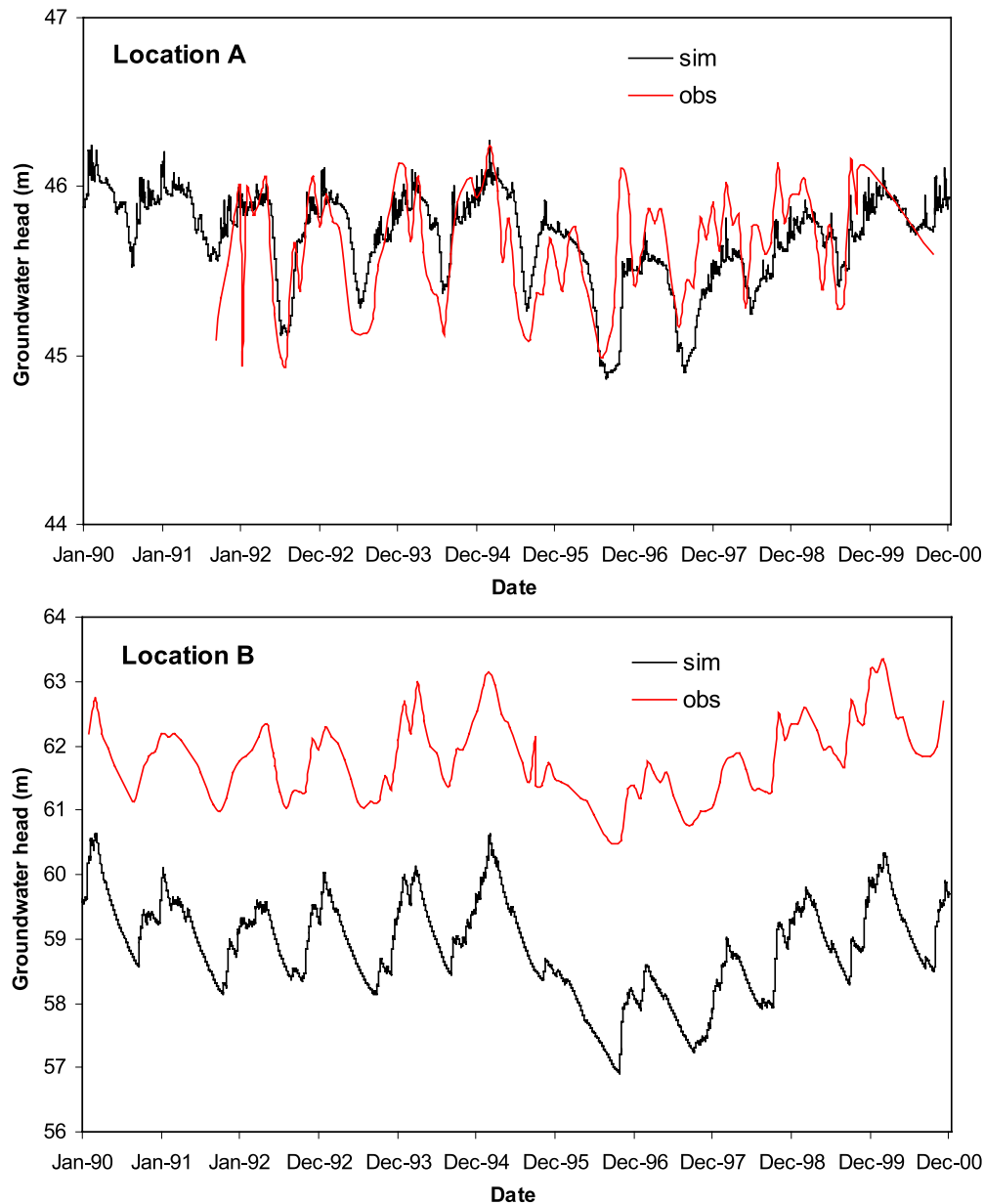


Figure 5. Observed and simulated groundwater heads at locations A and B in Figure 2.

the A2 scenario simulation, indicating that the hydrological response to the climate changes is only marginally affected by parameter value variations within the estimated parameter confidence intervals.

4. Results

[42] The changes in meteorological variables, irrigation, sea level, land use, and the transpiration response are expected to be among the most important factors for the hydrological system in a changing climate. In this section the hydrological and water management effects of climate change are presented separately, but also the combined effects are shown. The simulations are conducted in transient mode for the period 1971–2004, but only the period 1990–2004 is used for the detailed analysis because 1971–1989 is a spin-up period, where the model is allowed to adjust to the prevailing hydrological conditions.

4.1. Effects of Climate Change on the Hydrological System

4.1.1. Annual Water Balance

[43] The water balance provides a general insight into the changes in the hydrological cycle of the catchment as a result of climate change. In Table 3 the most important water balance components for the groundwater system are presented using climate input corresponding to current conditions and the A2 and B2 climate scenarios. Simulation results are shown for the cases where abstractions and irrigation are not included (Table 3, top) and included (Table 3, bottom). The results are spatially averaged, mean annual values for the 15-year period. The net recharge is defined as the outflow from the root zone minus the sum of evapotranspiration and net flow from the groundwater zone to the overland compartment for the grids where the soil profile is completely saturated and the unsaturated zone no longer active. The net horizontal boundary outflow is the

Table 3. Mean Annual Total Water Balance for the Current Climate and the Absolute and Relative Changes When Comparing the A2 and B2 Scenarios to the Current Climate^a

Scenario	Net Recharge	Horizontal Boundary Outflow	Drain Flow	Base Flow	Water Supply	Irrigation
<i>Simulations Not Including Abstractions and Irrigation</i>						
Current climate	550	23	279	252		
A2 scenario	+ 67 (12%)	+ 1 (4%)	+ 56 (20%)	+ 13 (5%)		
B2 scenario	+ 113 (21%)	+ 1 (4%)	+ 92 (33%)	+ 22 (9%)		
<i>Simulations Including Abstractions and Irrigation</i>						
Current climate	560	23	264	243	10	18
A2 scenario	+ 74 (13%)	0	+ 50 (19%)	0	0	+ 16 (89%)
B2 scenario	+ 118 (21%)	+ 1 (4%)	+ 84 (32%)	+ 20 (8%)	0	+ 9 (50%)

^aWater balance values are in millimeters. Relative changes are in parentheses.

net outflow across the catchment boundary and accounts primarily for groundwater flow to the sea. Drain flow includes drainage from groundwater to rivers and drainage to the sea in coastal regions. Base flow is the net flow of groundwater to rivers.

[44] Net recharge increases for both climate scenarios, which is of great interest because recharge drives the changes in the groundwater system and the stream discharges. Drain flow is the variable of the water balance that shows the largest absolute increases for the A2 and B2 climate scenarios. The increase in drain flow is the result of the groundwater levels reaching above the drain levels more often and in larger areas.

[45] Table 4 shows the spatially averaged, mean monthly recharge for the simulations that do not take abstractions and irrigation into account. The results for the simulations with abstractions and irrigation are not shown because the monthly recharge for the current climate is only 1–3 mm higher during the irrigation months than for the simulation without abstractions. The seasonal dynamics in recharge increase for both climate scenarios, with significant increases in the period from December to March and decreasing recharge during the late summer period from July to September. Of the two scenarios B2 shows the largest increase (Table 3, top) because of less increase in evapotranspiration during summer and higher precipitation in the last two months of the year in comparison to the A2 scenario (Figure 3).

4.1.2. Mean Groundwater Head

[46] Two numerical layers in the model are analyzed here: layer 1 which is the upper, unconfined aquifer and layer 5, the deeper, main aquifer in the area. For the current climate the spatially averaged, mean annual groundwater heads are 33.57 m and 33.49 m in layer 1 and 31.53 m and 31.28 m in layer 5 for the simulations not including and including abstractions, respectively. Including abstractions decreases the mean groundwater heads by 0.08 m in layer 1 and 0.25 m in layer 5. The impact of abstractions on groundwater heads for the current climate can be compared to the change in mean annual groundwater heads as a result of climate change. Table 5 shows the absolute changes in groundwater head for layers 1 and 5 for the two climate scenarios. The groundwater heads in layer 5 increase more than in layer 1 because in layer 1 the rise in groundwater level is restricted by the drains, which have been defined in the entire catchment at a depth of 0.5 m below ground surface. It can be seen that the effect of abstractions on groundwater heads for the current climate is smaller than the effect of climate change for layer 1 for both scenarios. On

the other hand, for layer 5 the increase of 0.17 m for the A2 scenario is smaller than the 0.25 m decrease owing to abstractions in the current climate, but this is because irrigation increases significantly for the A2 scenario (see Table 3, bottom). Corresponding to the larger increase in recharge, the B2 scenario also shows larger increases in mean annual groundwater heads.

[47] Figure 6 shows the spatial distribution of the absolute changes in mean groundwater heads for layer 5 when comparing the scenario to the current climate simulation and including abstractions. The results for layer 1 and the situation without abstractions are not shown because the spatial distribution is similar. A considerable variation in the changes in groundwater heads can be seen, controlled mainly by the distance from streams, the geology of the subsurface, and the depth to the groundwater table. The impact is largest in layer 5 for the B2 scenario, where 45% of the catchment area shows an increase between 0.25 and 1 m, and 7% of the area shows a rise in groundwater head above 1 m. In layer 1 for the A2 scenario about 25% of the catchment area shows an increase in groundwater head above 0.25 m (not shown).

[48] The spatially averaged, mean groundwater heads in layer 1 are compared for the end of the winter (January to March) and late summer (August to October) for the current climate and the two climate scenarios. The results show that the seasonal amplitude increases by 40–50% (e.g., from 0.7 m in the current climate to 1 m for the A2 scenario including abstractions). This is mainly due to the increase in groundwater heads during the winter months, whereas the late summer values show no change for the A2 scenario and slight increases for the B2 scenario when compared to the current climate. Even though the spatially averaged values for the whole catchment show no to little change in summer, locally decreases in groundwater heads up to 0.5 m occur.

4.1.3. Stream Discharge

[49] The rising groundwater levels result in increases in mean annual stream discharges because of increasing base flow and drain flow, where the latter is due to the longer

Table 4. Spatially Averaged, Mean Monthly Recharge for the Current Climate and the A2 and B2 Scenarios for the Simulation Without Abstractions and Irrigation^a

Scenario	Jan	Feb	Mar	Apr	May	Jun	Jul	Aug	Sep	Oct	Nov	Dec
Current	101	85	59	13	−6	−4	−1	6	39	79	84	97
A2	145	132	73	10	−10	−7	−6	−8	4	75	92	123
B2	137	119	75	16	−6	−6	−6	−5	21	74	110	141

^aValues are in millimeters.

Table 5. Absolute Changes in Spatially Averaged, Mean Annual Groundwater Heads When Comparing the A2 and B2 Scenarios to the Current Climate for the Simulations Not Including and Including Abstractions and Irrigation^a

	A2 Scenario		B2 Scenario	
	n.a.	i.a.	n.a.	i.a.
Upper unconfined aquifer (numerical layer 1)	0.19	0.17	0.32	0.30
Main aquifer (numerical layer 5)	0.28	0.17	0.45	0.39

^aValues are in meters; n.a., not including abstractions and irrigation; i.a., including abstractions and irrigation.

time and larger area where groundwater levels rise above the drain levels. Table 6 shows the mean discharges at six discharge stations (Figure 2) for the current climate and the A2 and B2 scenarios. For the three stations with the largest catchment area (25.14, 25.11, and 31.13) the A2 scenario without abstractions results in a relative increase around 13%, whereas the B2 scenario results in an increase around 21%. Especially for the A2 scenario the inclusion of abstractions and irrigation results in smaller relative increases in discharge with increases around 10%, while for the B2 scenario, with an increase of 20%, the effect of increased irrigation on stream discharges is small. As a result of the increased dynamics in recharge (Table 4) it can be expected that seasonal changes in stream discharge occur as well. Figure 7 shows the mean monthly discharges simulated at discharge stations 25.14 and 25.37 at the downstream and upstream end of the Skjern River, respectively. Large absolute increases occur during the winter months, but also relatively large decreases during the late summer months are seen, with the A2 scenario resulting in the largest decreases.

4.2. Effects of Climate Change on Irrigation

[50] The soil moisture storage for each month, spatially averaged for the whole catchment is extracted for the simulation without abstractions and irrigation to determine whether drier conditions occur during summer for the

climate scenarios owing to the decrease in precipitation and the increase in potential evapotranspiration for these months (results not shown). From March to September soil moisture storage decreases for both climate scenarios compared to the current climate, whereas it increases from October to February. Especially in August a significant change occurs, where soil moisture continues to decrease for both climate scenarios, whereas it remains constant in the current climate. This indicates that significantly more drying occurs toward the end of the summer as a result of climate change. Most of the soils in the catchment area are sandy and the drying effect on such soils will be most pronounced. Irrigation demand is therefore expected to increase considerably in the catchment for the climate change scenarios considered here.

[51] For the current climate the mean annual irrigation volume equals 99 Mm³, of which 45 Mm³ is used for irrigation of grain and 54 Mm³ for grass. These volumes correspond to an irrigation depth of 15 mm for grain and 35 mm for grass. The total mean annual irrigation increases to 187 Mm³ and 148 Mm³ for the A2 and B2 scenario, respectively, corresponding to relative increases of 89% and 50% (see Table 3, bottom). The increase in irrigation depth is 33 mm (94%) and 18 mm (51%) for grass and 13 mm (86%) and 7 mm (48%) for grain for the A2 and B2 scenario, respectively.

[52] Figure 8 shows the total mean annual irrigation volume for the period 1990–2004 for the current climate and both scenarios. The largest absolute increase in annual irrigation equals 173 Mm³ for the A2 scenario and occurs in 1996, which already showed a large irrigation volume for the current climate. For years where less irrigation is needed in the current climate large increases are predicted for future conditions.

[53] Figure 9 shows the mean monthly irrigation volume for the current climate and both scenarios. The largest absolute increases in monthly irrigation occur in August, namely 17 mm and 11 mm for the A2 and B2 scenario, respectively. This results in a shift in the peak irrigation month from July to August for grass, but not for grain because irrigation is stopped in the middle of August when grain is harvested. September and October show very high

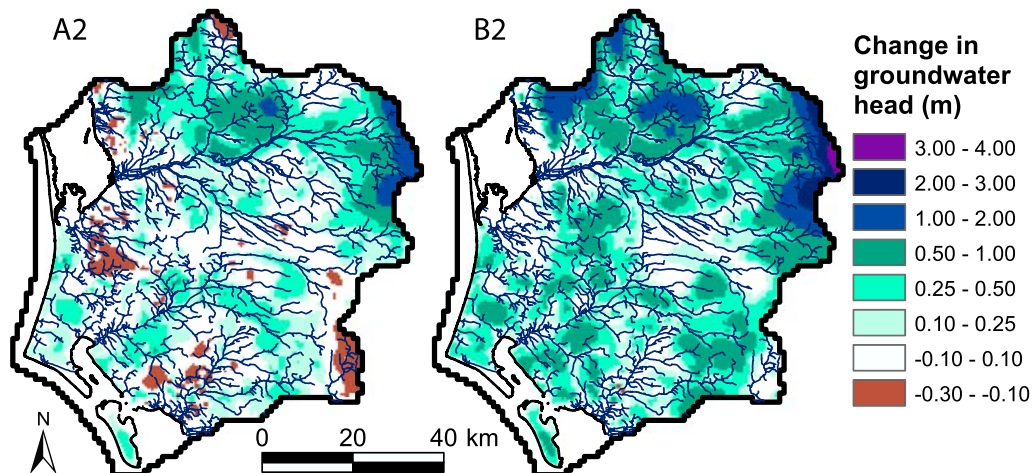


Figure 6. Change in mean groundwater head when comparing the A2 and B2 scenario to the current climate for model layer 5 (including abstractions and irrigation).

Table 6. Simulated Mean Daily Discharges at the Discharge Stations for the Current Climate and A2 and B2 Scenarios for the Simulations Not Including and Including Abstractions and Irrigation^a

Scenario	Discharge Stations											
	25.11		31.13		35.03		25.14		25.37		25.08	
	n.a.	i.a.	n.a.	i.a.	n.a.	i.a.	n.a.	i.a.	n.a.	i.a.	n.a.	i.a.
Current	9.1	8.6	13.7	13.0	3.5	3.3	24.1	23.1	0.9	0.8	1.5	1.3
A2	10.3	9.5	15.5	14.2	3.9	3.6	27.3	25.5	1.1	1.0	1.7	1.4
B2	11.0	10.4	16.6	15.5	4.1	3.9	29.0	27.5	1.2	1.1	1.8	1.6

^aValues are in m³/s.

relative increases in irrigation. Table 3 (bottom) shows that the abstractions for households, industry, and irrigation as a whole, only constitute a small part of the annual mean water balance. The absolute differences in mean groundwater heads and discharges are therefore not very large when comparing the simulations including and not including abstractions and irrigation. However, since the irrigation water is primarily abstracted in the period June to September, where the net recharge is low or even negative (Table 4), it results in a pronounced impact on base flow to streams. The mean monthly discharges during the summer months are a few percent lower when abstractions and irrigation are considered and the impact is further exacerbated in the scenario runs.

4.3. Effects of Sea Level Rise

[54] The effects of an increase in sea level of 0.5 m and 1 m are investigated. The areas flooded as a result of the sea level rise are relatively small, but the rise in sea level is

expected to not only affect these areas, but also to influence groundwater levels further inland. Figure 10 shows the change in mean groundwater head in layer 5, when comparing the simulation including 1 m sea level rise to the simulation without sea level rise for the A2 scenario. The sea level rise influences the groundwater heads up to 10 km inland along the coast. The affected area is similar for the 0.5 m sea level rise simulation, but the increases are smaller. The effect of sea level rise is significant for low-lying areas, where the simulated increase in groundwater levels for the A2 scenario is up to 0.5 m and 0.2 m for the 1 m and 0.5 m sea level rise scenarios, respectively. The values presented in Figure 10 only show the effect of the rise in sea level and should thus be added to the increase in groundwater levels (Figure 6) owing to the changes in meteorological input.

4.4. Effects of Land Use Changes

[55] Land use changes can affect the water balance in a watershed owing to differences in the evaporative properties

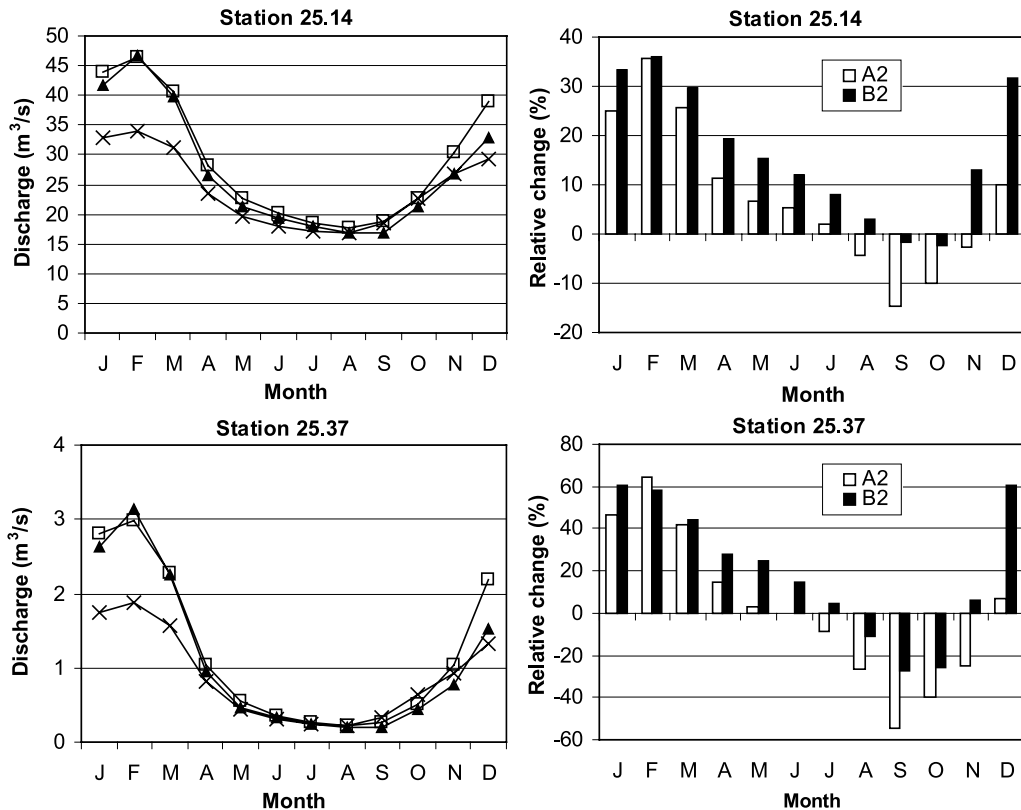


Figure 7. Monthly mean discharge for the current climate (crosses), the A2 scenario (triangles), and the B2 scenario (squares) for the simulations including abstractions and irrigation.

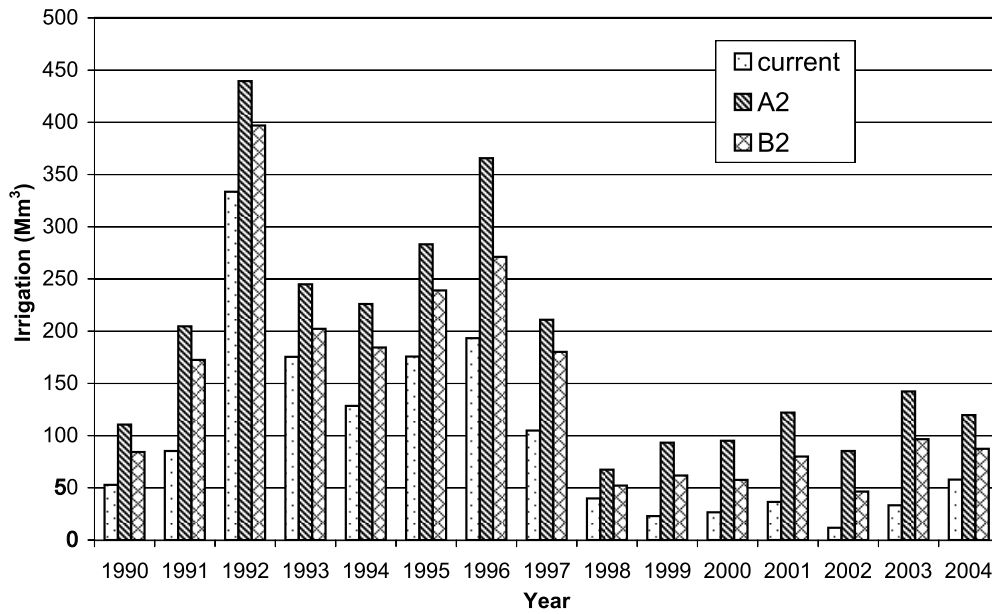


Figure 8. Total mean annual irrigation for the current climate and the A2 and B2 scenarios.

of the vegetation. Potential evapotranspiration ET_p in the model is described as ET_{ref} multiplied by a crop factor K_c . Forests have the highest ET_p because the K_c value is the highest throughout the year, namely 1.2 (Table 2). It is however less clear how large the differences are in actual evapotranspiration ET_{act} because this is not only determined by the crop factor, but also by the LAI, root depth, and water availability. To quantify what the effects of land use changes are, the different components of annual ET_{act} for forest, grain, and grass are compared (Table 7). Total ET_{act} includes evaporation from canopy interception E_{can} , transpiration from the unsaturated and saturated zone, evaporation of ponded water, and snow ablation. The contributions of the latter three are however small. For the current climate simulated mean annual ET_{act} for forest is 8% higher than for grain and 15% higher than for grass. The higher ET_{act} for forest is mainly due to the relatively high E_{can} which is a result of the large LAI used for forest. When comparing the A2 scenario to current climate ET_{act} increases by 10% for grain and grass and by 9% for forest. The relative contri-

bution of each evaporation component does not change significantly for the A2 scenario.

[56] To study the effects of land use changes, a subcatchment is selected, encompassing the upstream part of the Skjern River catchment (Figure 1). The size of the subcatchment is 1038 km². The land use distribution is 61% grain, 2% urban, 18% grass, 6% heather, and 13% forest. A policy

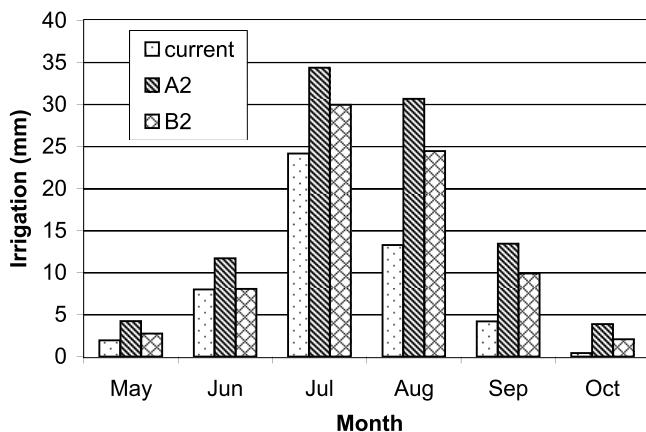


Figure 9. Total mean monthly irrigation (mm) for the current climate and the A2 and B2 scenarios.

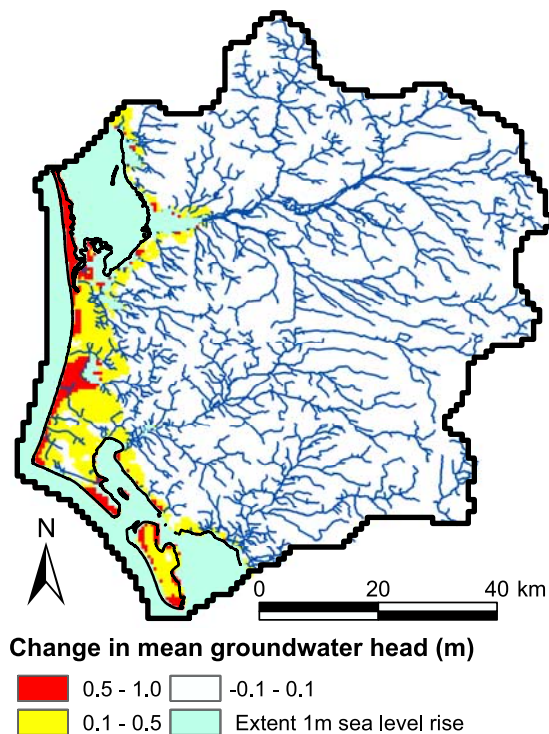


Figure 10. Change in mean groundwater head (m) for layer 5 when comparing the simulation with 1 m sea level rise to the simulation with current mean sea level for the A2 scenario.

Table 7. Absolute and Relative Contribution to Annual Actual Evapotranspiration for Land Use Types Grain, Grass, and Forest for the Current Climate^a

	E_{can}	E_{pon}	E_{uz}	E_{sz}	E_{snow}	Total
Grain	96 (19%)	5 (1%)	373 (74%)	23 (5%)	7 (1%)	504
Grass	111 (23%)	4 (1%)	337 (71%)	15 (3%)	7 (2%)	474
Forest	162 (30%)	2 (0%)	360 (66%)	13 (2%)	8 (2%)	545

^aValues are in millimeters. E_{can} , evaporation from canopy interception; E_{pon} , evaporation of ponded water transpiration; E_{uz} , transpiration from unsaturated zone; E_{sz} , transpiration from saturated zone; E_{snow} , snow ablation.

of the Danish government is to double the forested area in Denmark within the next 80 to 100 years. To quantify the effects of such a land use change, all cells with land use class grass in the subcatchment are changed to forest, increasing the forested area to 230% of the original area. As a comparison another simulation is carried out where an area of equal size with grain is changed to forest and the grass area remains at 18% of the subcatchment area. Figure 11 shows the mean monthly ET_{act} for the grass-to-forest and no-land-use-change scenarios, for the current climate and the A2 scenario. It can be seen that changing the land use from grass to forest increases the ET_{act} considerably from May to July, though the increase due to climate change (A2 scenario) is larger.

[57] When grass is changed to forest, the average recharge in the current climate is reduced from 562 mm/a to 546 mm/a, corresponding to a relative decrease of 3%. When grain is changed to forest, the recharge decreases with 2% to 551 mm/a. The relative change in recharge due to the doubling of forest area remains the same for the climate scenarios, reducing for example the recharge in the A2 scenario from 640 mm/a to 620 mm/a and 625 mm/a for the grass-to-forest and grain-to-forest scenarios, respectively. These simulation results suggest that changing the land use to forest can only slightly counteract the increase in recharge due to climate change.

4.5. Effects of Changes in Crop Growth Dates and Evapotranspiration Response

[58] In a changing climate it is very uncertain whether and how the ET properties of the crops will change and also how crop management practices are adapted. It is thought that a warmer climate and changes in soil water content will shift sowing and planting dates and change crop development times, generally leading to faster development, including earlier flowering [Chmielewski *et al.*, 2004] and earlier sowing of spring crops [Olesen, 2005]. Here the effect of changes in the crop dates and development times on the hydrology in the watershed is studied by shifting the sowing date for grain from 1 April in the current climate to 15 March for the scenario climate. The crop development time is shortened by 5 days, resulting in the maximum values occurring from day 55 to day 130 and harvest on 24 July. For grass in the scenario climate the first cut occurs 5 days earlier than in the current climate and the last cut occurs ten days later.

[59] The results for the A2 scenario with changed sowing and crop development dates are compared to the A2 scenario simulation with the current dates. A change in the cropping dates only has a slight effect on the mean

annual recharge, namely an increase of 5 mm. The largest decreases in mean monthly recharge are about 2 mm and occur in March and April. September and October show slight increases, 5 mm and 3 mm, respectively, which is a result of the soil moisture content increasing sooner as a result of the earlier harvesting of grain.

[60] Apart from a shift in crop development dates, a plausible scenario is that the evaporative properties of plants change because plant respiration becomes more water efficient with increasing CO_2 concentrations [Kruijt *et al.*, 2008]. This scenario is investigated by assuming that ET_{ref} for the A2 scenario can be approximated by the input for the current climate (Figure 3). This results in a significant increase in mean annual recharge of 47 mm, when compared to the 67 mm increase for the original A2 scenario (Table 3, top). This will result in even higher groundwater levels and stream discharges, especially in summer. However, a more careful analysis of this problem is required to produce reliable results, which is beyond the purpose of the present study.

5. Discussion

[61] The results from the various scenario simulations in this study can be used to quantitatively compare the effects of climate and land use change in an agricultural watershed. To facilitate the discussion of the results Table 8 includes the absolute change in key hydrological variables for the scenario simulations. The first row in Table 8 (run 1) shows the baseline absolute values for the current climate simulation not including abstractions for water supply and irrigation (current-n.a.).

[62] Generally, the A2 and B2 simulations (runs 3 and 8) show that recharge to groundwater increases considerably owing to climate change even though actual evapotranspiration also increases substantially. This is because most of the precipitation increase occurs during the winter months, when evaporative demand is low and the soils are saturated. The increase in recharge results in increases in mean annual

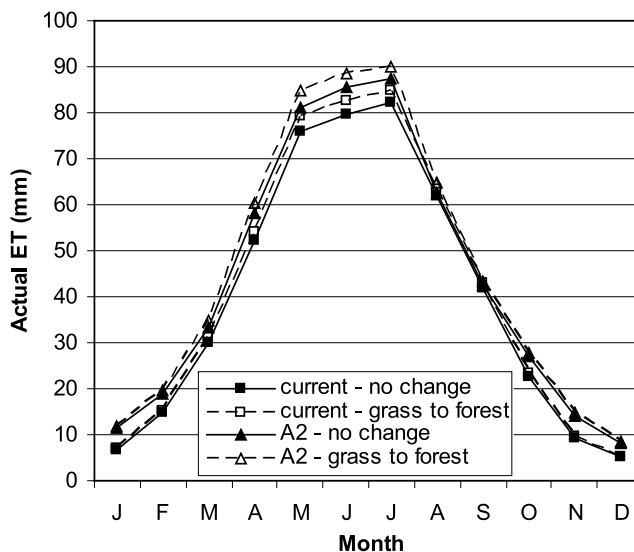


Figure 11. Mean monthly actual evapotranspiration for the grass-to-forest and the no-land-use-change scenarios for the current climate and the A2 scenario.

Table 8. Absolute Changes in Key Hydrological Variables for the Various Climate and Land Use Change Simulations^a

Run	Description	ET _{act} (mm)	Recharge (mm)	Heads L1 (m)	Heads L5 (m)	Q _{Feb} (m ³ /s)	Q _{Sep} (m ³ /s)
1	current n.a.	492	550	33.6	31.7	33.97	18.54
2	current i.a. ^b	+ 14	+ 10	− 0.09	− 0.25	− 1.12	− 1.16
3	A2 n.a. ^b	+ 49	+ 67	+ 0.19	+ 0.28	+ 12.83	− 1.55
4	A2 i.a. ^c	+ 35	+ 17	− 0.10	− 0.36	− 2.22	− 2.18
5	A2 shift dates ^c	− 5	+ 5	+ 0.01	+ 0.02	+ 0.31	+ 0.15
6	A2 no increase ET ^c	− 48	+ 47	+ 0.12	+ 0.16	+ 2.73	+ 0.95
7	A2 2× forest ^{c,d}	+ 19	− 20	na ^e	na ^e	na ^e	na ^e
8	B2 n.a. ^b	+ 45	+ 113	+ 0.32	+ 0.45	+ 12.44	+ 0.29
9	B2 i.a. ^f	+ 25	+ 15	− 0.11	− 0.32	− 1.74	− 1.72

^aThe first row shows the baseline absolute values for the current climate simulation not including abstractions for water supply and irrigation (current n.a.). A2 and B2 indicate the two climate scenarios, and i.a. means including abstractions.

^bCompared to current climate simulation without abstractions.

^cCompared to A2 scenario simulation without abstractions.

^dSpatially averaged for the subcatchment where land use was changed from grass to forest.

^eNot available for whole catchment.

^fCompared to B2 scenario simulation without abstractions.

groundwater levels up to 0.45 m (B2 scenario). Additionally, seasonal fluctuations will be larger with higher groundwater levels in winter and spring especially. Observed groundwater heads for the period 1970–2004 at four wells in the upper, unconfined aquifer of the catchment showed standard deviations of the order of 0.5–1 m. The simulated effect of climate change up to 0.45 m is smaller than the historic, natural variability at these wells but can be considered significant because 0.45 is a spatially averaged value for the whole catchment. Most areas in the catchment would not be affected by such increases because the present groundwater levels are at least a few meters below the ground surface. However, a larger part of the low-lying areas will be affected by groundwater flooding [Finch *et al.*, 2004] and generally for a longer period of time in winter and early spring. This may impact agricultural practice since it will be difficult to cultivate the soils using heavy machinery in the wet periods.

[63] The increase in seasonal dynamics in streamflow will have an impact on the low flow period in smaller streams, where the flow can drop below the minimum ecological flow, as defined in the water framework directive, during extremely dry years. However, a limitation of this study on the effects of climate change on extreme flows is the use of the delta change method because this method does not include changes in the variability of precipitation. The large increase in stream discharge during winter time is expected to have several implications. Thodsen *et al.* [2008] showed that sediment transport in a tributary to Varde Stream may increase by up to 17% for the A2 scenario as a result of increasing winter discharge. In a study by Mikkelsen [2008] the flooding risk in the Stora River, located just north of the Skjern River catchment, increased significantly for the A2 scenario. In the catchment considered in this study no larger cities are located in the larger stream valleys and the socioeconomic impacts may therefore not be significant. However, the changes may have severe agricultural and recreational implications.

[64] The results of the land use change scenarios (Table 8, runs 5 and 7) show that the simulated land use changes and shift in cropping dates only affect the hydrology of the watershed marginally compared to climate change. For example, the increase in groundwater recharge due to climate change equals 67 mm and 113 mm for the A2

and B2 scenario, respectively. When doubling the area with forest by changing grass to forest for the A2 scenario, the increase in recharge is 20 mm less than for the A2 scenario with current land use. The sensitivity of the hydrological system to changes in land use, for example afforestation, is closely related to the parameters assigned to the vegetation. The values for LAI, root depth and crop factor found in the literature vary considerably, which makes the simulation of land use change subjective to the choice of parameters included in the model. A best estimate was included for the vegetation properties in this study, but the uncertainty of these parameters increases the uncertainty in the simulated changes in evapotranspiration.

[65] The simulation used to study the CO₂ effect on transpiration (Table 8, run 6), shows that recharge increases considerably, namely 47 mm, compared to the 67 mm increase for the baseline A2 scenario, resulting in a total increase of 114 mm. Groundwater levels also increase, but stream discharges do not increase as much. This shows that the increase in stream discharge due to climate change for a large part is a result of the increase in winter precipitation yielding higher drain flow and to a lesser extent due to an increase in base flow. Drain flow represents flow through drain pipes and ditches and in smaller streams, which cannot be represented in the model because of the large grid size.

[66] The stomatal “antitranspirant” response of plants to rising atmospheric CO₂ is included in a simplified manner here, but CO₂ is also a plant fertilizer, which could result in an increase in foliage area. A limitation of this study is therefore that vegetation is not simulated dynamically, hereby excluding the feedback of vegetation structure on the water balance of the land surface. By using empirical crop factors, changes in vegetation properties are not included and the applicability of these factors for calculating ET in a changing climate is therefore questionable. Another complicating factor is that the baseline ET data for the current climate are calculated using the empirical Makkink formula [Makkink, 1957], whereas the delta change values (relative change in ET for future climate scenarios) are calculated from ET values estimated using the FAO Penman-Monteith equation [Allen *et al.*, 1998]. All in all, potential evapotranspiration estimates are very uncertain in future climate change simulations.

[67] Irrigation constitutes a relatively small part of the total water balance in the catchment, but increases substantially from 99 Mm³ for the current climate to 187 Mm³ (89%) for the A2 scenario. As a result, the mean annual groundwater level in layer 5 for the A2 scenario (Table 8, run 4) decreases more, due to the abstractions for irrigation (−0.36 m), than it increases as a result of climate change (+0.28 m). Locally, this can have an effect on groundwater levels and thus on wetlands and stream discharges because the abstractions are concentrated in a short period of the year and are largest during July and August (Figure 9), which are expected to be drier and warmer under future climate conditions (Figure 3). However, on the basis of the results of this study no clear conclusions can be drawn with respect to the sustainability of increasing groundwater abstraction for irrigation in a future climate because it depends on other factors like land use and the impact of increasing CO₂ concentrations on transpiration.

[68] This study focuses on the change in simulated results because the uncertainty of the changes is much smaller than the uncertainty of the absolute values because the models are highly correlated. Nevertheless, the results are subject to large uncertainties related to the model formulation of the climate models, the transfer method, and the hydrological model structure and these uncertainties are very difficult to quantify. First of all, the forcing GCM has a considerable effect on the RCM simulation, for example on the simulated precipitation in the RCM through the large-scale circulation forced by the GCM. *Graham et al.* [2007b] found that the choice of GCM (HadAM3H or ECHAM4/OPYC3) had a larger impact on changes in river discharges in northern Europe than the selection of either the SRES A2 or B2 scenario or the choice of RCM. In this study the RCM is forced by only one GCM, limiting the possibility to determine the effect of the choice of GCM on the simulated meteorological variables. *Christensen and Christensen* [2007] mention natural climate variability as another source of uncertainty, resulting in the necessity of using GCM experiments involving ensemble integrations to provide a more exhaustive sample of possible future climates.

[69] The future GHG concentrations form a large uncertainty, which is only partly approached in this study by comparing two scenarios in the medium category of cumulative emissions, as defined by the *IPCC* [2000], with the B2 scenario in the lower end and the A2 scenario in the higher end of this category. It is not the purpose of the present paper to cover the full range of plausible future climates, but to study the sensitivity of the groundwater system to different climate change scenarios. For Denmark the scenarios result in a 2.2° and 3.1° increase in temperature for the B2 and A2 scenario, respectively, when comparing the period 2071–2100 to 1961–1990. Currently, no RCM results are available for Denmark for the most extreme SRES marker scenarios, but at a global scale the B1 scenario shows the smallest global surface warming of these scenarios and the temperature increase is 0.6° lower than that for the B2 scenario toward 2100 [*IPCC*, 2007]. The A1FI shows the largest increase in temperature and is 0.6° higher than for the A2 scenario. The full range of increase in temperature for Denmark can then be estimated to be between 1.6 and 3.7°, though this estimation is based on the assumption that the differences between the SRES

scenarios at the global scale are equal to the differences at the regional scale for Denmark.

[70] The sources of uncertainty related to the hydrological model include input data, model parameter values, and model structure. Here the sensitivity of parameter uncertainty on the impact of climate changes was assessed. The investigated parameters were shown to have a significant effect on the groundwater head predictions, but little change in stream discharges was found. However, when changes between model results using different climate scenarios were analyzed, the parameter uncertainty only showed a minor effect on the relative impact. Hence this indicates that the results are robust to the parameter uncertainty. Model structure uncertainty may yield a more pronounced effect on the predictions but was beyond the scope of the present study to quantify. However, when comparing to results from other types of hydrological impact models (e.g., *Andersen et al.* [2006] and *Thodsen* [2007] using lumped rainfall-runoff models) the results for the changes in stream discharge seem relatively robust toward the type of model being applied.

[71] As a result of all these uncertainties, climate change impact studies should be seen as a tool to study processes in the catchment and to determine the sensitivity of the hydrological system to changes in climate and other characteristics, such as land use. In this catchment the most significant changes are due to the increases in precipitation during the winter months, though the increase in actual evapotranspiration is significant as well. A large-scale study including a more advanced vegetation module would be of great added value to the process understanding of the effects of climate change. This would also make it possible to represent land use changes in more detail.

6. Conclusions

[72] This paper presents a quantitative comparison of possible climate and land use change impacts on the hydrology of a large-scale agricultural catchment in Denmark. The climate change impacts were simulated by using climate-forcing data for the SRES A2 and B2 scenarios for the period 2071–2100 and by raising the sea level to +0.5 and +1 masl. The land use change effects included the doubling of the area with forest at the expense of grain and grass, changes in crop development dates, and a limited increase in potential evapotranspiration for crops in the scenario climate simulations. Hydrological model output, such as the water balance, groundwater heads, stream discharges, irrigation volumes, and actual evapotranspiration, was compared for a 15-year period.

[73] This study has shown that climate change has the most substantial effect on the hydrology in this catchment. Both the A2 and the B2 climate scenarios showed significant impacts on the hydrological system with large increases in winter precipitation resulting in higher recharge and groundwater levels. However, the A2 scenario with higher evapotranspiration and lower precipitation during summer than the B2 scenario resulted in depletion of summer stream discharges. This illustrates that the uncertainty in GHG emissions scenarios translates into a corresponding uncertainty for the hydrological system. Other factors such as irrigation and CO₂ effects on transpiration had a smaller, but significant impact on the hydrological system as well. Increasing irrigation demands

resulted in reductions in groundwater levels and stream discharges whereas the “antitranspirant” CO₂ effect showed increases in groundwater recharge and stream discharges. Also, sea level rise was shown to have a significant effect on groundwater levels, however only in coastal areas. The shift in growing season and the land use changes included here affected the water balance to a lesser extent.

[74] The simulated hydrological effects of climate and land use change are subject to large uncertainties related to the climate change scenarios and corresponding output from climate models, but also the land use scenarios and the changes in vegetation properties. A more advanced representation of the vegetation’s adaptation to changing CO₂ concentrations and changes in cropping pattern and crop development stages would greatly improve future work. Moreover, to accurately simulate the combined effects of climate change and land use change a direct coupling between the hydrological model and the climate model is necessary. In this way feedback processes such as latent heat flux from soil moisture and vegetation to the atmosphere are included. A direct coupling would also make it possible to carry out a more comprehensive study on the impact of changes in hydrological extremes, which is not included in this study because the transfer method for the climate data sets is based on the variability of the current climate. Last but not least, this would also facilitate the use of multiple GCMs and climate scenarios, which is necessary to cover the scope of uncertainties related to climate model output.

[75] **Acknowledgments.** The authors wish to thank the Danish Water and Wastewater Association and Copenhagen Energy for their financial support to this study.

References

- Allen, D. M., D. C. Mackie, and M. Wei (2004), Groundwater and climate change: A sensitivity analysis for the Grand Forks aquifer, southern British Columbia, Canada, *Hydrogeol. J.*, *12*(3), 270–290, doi:10.1007/s10040-003-0261-9.
- Allen, R. G., L. S. Pereira, D. Raes, and M. Smith (1998), *Crop Evapotranspiration: Guidelines for Computing Crop Water Requirements*, FAO Irrig. Drain. Pap., vol. 56, 290 pp., Food and Agric. Org. of the U. N., Rome.
- Allerup, P., H. Madsen, and F. Vejen (1998), Standard values (1961–90) for precipitation correction (in Danish), *Tech. Rep. 98–10*, 64 pp., Dan. Meteorol. Inst., Copenhagen.
- Andersen, H. E., B. Kronvang, S. E. Larsen, C. C. Hoffmann, T. S. Jensen, and E. K. Rasmussen (2006), Climate-change impacts on hydrology and nutrients in a Danish lowland river basin, *Sci. Total Environ.*, *365*, 223–237, doi:10.1016/j.scitotenv.2006.02.036.
- Anderson, M. P., and W. W. Woessner (1992), *Applied Groundwater Modeling*, Academic, San Diego, Calif.
- Andréasson, J., S. Bergström, B. Carlsson, L. P. Graham, and G. Lindström (2004), Hydrological change: Climate change impact simulations for Sweden, *Ambio*, *33*, 228–234, doi:10.1639/0044-7447(2004)033[0228:HCCIS]2.0.CO;2.
- Arnell, N. W. (1999), The effect of climate change on hydrological regimes in Europe: A continental perspective, *Glob. Environ. Change*, *9*(1), 5–23, doi:10.1016/S0959-3780(98)00015-6.
- Bindoff, N. L., et al. (2007), Observations: Oceanic climate change and sea level, in *Climate Change 2007: The Physical Science Basis: Contribution of Working Group I to the Fourth Assessment Report of the IPCC*, edited by S. Solomon et al., pp. 385–432, Cambridge Univ. Press, New York.
- Bourouai, F., G. Vachaud, L. Z. X. Li, H. Le Treut, and T. Chen (1999), Evaluation of the impact of climate changes on water storage and groundwater recharge at the watershed scale, *Clim. Dyn.*, *15*(2), 153–161, doi:10.1007/s003820050274.
- Brouyère, S., G. Carabin, and A. Dassargues (2004), Climate change impacts on groundwater resources: Modeled deficits in a chalky aquifer, Geer basin, Belgium, *Hydrogeol. J.*, *12*(2), 123–134, doi:10.1007/s10040-003-0293-1.
- Caballero, Y., S. Voirin-Morel, F. Habets, J. Noilhan, P. LeMoigne, A. Lehenaff, and A. Boone (2007), Hydrological sensitivity of the Adour-Garonne river basin to climate change, *Water Resour. Res.*, *43*, W07448, doi:10.1029/2005WR004192.
- Chmielewski, F.-M., A. Müller, and E. Bruns (2004), Climate changes and trends in phenology of fruit trees and field crops in Germany, 1961–2000, *Agric. For. Meteorol.*, *121*, 69–78, doi:10.1016/S0168-1923(03)00161-8.
- Chow, V. T., D. R. Maidment, and L. W. Mays (1988), *Applied Hydrology*, McGraw-Hill, New York.
- Christensen, J. H., and O. B. Christensen (2007), A summary of the PRUDENCE model projections of changes in European climate by the end of this century, *Clim. Change*, *81*, suppl. 1, 7–30, doi:10.1007/s10584-006-9210-7.
- Christensen, J. H., O. B. Christensen, P. Lopez, E. van Meijgaard, and M. Botzet (1996), The HIRHAM4 regional atmospheric climate model, *Sci. Rep. 96–104*, 51 pp., Dan. Meteorol. Inst., Copenhagen.
- Christensen, N. S., A. W. Wood, N. Voisin, D. P. Lettenmaier, and R. N. Palmer (2004), The effects of climate change on the hydrology and water resources of the Colorado river basin, *Clim. Change*, *62*, 337–363, doi:10.1023/B:CLIM.0000013684.13621.1f.
- Christensen, O. B., and J. H. Christensen (2004), Intensification of extreme European summer precipitation in a warmer climate, *Global Planet. Change*, *44*(1–4), 107–117, doi:10.1016/j.gloplacha.2004.06.013.
- Christensen, O. B., J. H. Christensen, B. Machenhauer, and M. Botzet (1998), Very high-resolution regional climate simulations over Scandinavia: Present climate, *J. Clim.*, *11*(12), 3204–3229, doi:10.1175/1520-0442(1998)011<3204:VHRRCS>2.0.CO;2.
- Déqué, M., et al. (2005), Global high resolution versus limited area model climate change projections over Europe: Quantifying confidence level from PRUDENCE results, *Clim. Dyn.*, *25*(6), 653–670, doi:10.1007/s00382-005-0052-1.
- Déqué, M., D. P. Rowell, D. Lüthi, F. Giorgi, J. H. Christensen, B. Rockel, D. Jacob, E. Kjellström, M. De Castro, and B. van den Hurk (2007), An intercomparison of regional climate simulations for Europe: Assessing uncertainties in model projections, *Clim. Change*, *81*, suppl. 1, 53–70, doi:10.1007/s10584-006-9228-x.
- DHI (2007), *MIKE SHE User Manual Volume 2: Reference Guide*, Hoersholm, Denmark.
- Finch, J. W., R. B. Bradford, and J. A. Hudson (2004), The spatial distribution of groundwater flooding in a chalk catchment in southern England, *Hydrol. Processes*, *18*(5), 959–971, doi:10.1002/hyp.1340.
- Graham, D. N., and M. B. Butts (2006), Flexible, integrated watershed modelling with MIKE SHE, in *Watershed Models*, edited by V. P. Singh and D. K. Frevert, pp. 245–272, Taylor and Francis, Boca Raton, Fla.
- Graham, L. P., J. Andréasson, and B. Carlsson (2007a), Assessing climate change impacts on hydrology from an ensemble of regional climate models, model scales and linking methods: A case study on the Lule River basin, *Clim. Change*, *81*, suppl. 1, 293–307, doi:10.1007/s10584-006-9215-2.
- Graham, L. P., S. Hagemann, S. Jaun, and M. Beniston (2007b), On interpreting hydrological change from regional climate models, *Clim. Change*, *81*, suppl. 1, 97–122, doi:10.1007/s10584-006-9217-0.
- Harrar, W. G., T. O. Sonnenborg, and H. J. Henriksen (2003), Capture zone, travel time, and solute-transport predictions using inverse modeling and different geological models, *Hydrogeol. J.*, *11*(5), 536–548, doi:10.1007/s10040-003-0276-2.
- Havnø, K., M. N. Madsen, and J. Dørgé (1995), MIKE 11: A generalized river modelling package, in *Computer Models of Watershed Hydrology*, edited by V. P. Singh, pp. 733–782, Water Res. Publ., Highlands Ranch, Colo.
- Hay, L. E., R. L. Wilby, and G. H. Leavesley (2000), A comparison of delta change and downscaled GCM scenarios for three mountainous basins in the United States, *J. Am. Water Resour. Assoc.*, *36*, 387–398, doi:10.1111/j.1752-1688.2000.tb04276.x.
- Henriksen, H. J., and A. B. Sonnenborg (2003), The freshwater cycle (in Danish), NOVA theme report, 266 pp., Geol. Surv. of Denmark and Greenland, Copenhagen.
- Henriksen, H. J., and T. O. Sonnenborg (2005), Accuracy criteria, in *Handbook of Groundwater Modeling (in Danish)*, GEUS Rep. 2005/80, chap. 12, 21 pp., Geol. Surv. of Denmark and Greenland, Copenhagen.
- Henriksen, H. J., L. Trolborg, P. Nyegaard, T. O. Sonnenborg, J. C. Refsgaard, and B. Madsen (2003), Methodology for construction,

- calibration and validation of a national hydrological model for Denmark, *J. Hydrol.*, 280, 52–71, doi:10.1016/S0022-1694(03)00186-0.
- Intergovernmental Panel on Climate Change (IPCC) (2000), *Special Report on Emissions Scenarios (SRES): A Special Report of Working Group III of the Intergovernmental Panel on Climate Change*, 570 pp., Cambridge Univ. Press, Cambridge.
- Intergovernmental Panel on Climate Change (IPCC) (2007), Summary for policymakers, in *Climate Change 2007: The Physical Science Basis: Contribution of Working Group I to the Fourth Assessment Report of the IPCC*, edited by S. Solomon et al., 18 pp., Cambridge Univ. Press, New York.
- Jyrkama, M. I., and J. F. Sykes (2007), The impact of climate change on spatially varying groundwater recharge in the grand river watershed (Ontario), *J. Hydrol.*, 338, 237–250, doi:10.1016/j.jhydrol.2007.02.036.
- Kleinn, J., C. Frei, J. Gurtz, D. Luthi, P. L. Vidale, and C. Schar (2005), Hydrologic simulations in the Rhine basin driven by a regional climate model, *J. Geophys. Res.*, 110, D04102, doi:10.1029/2004JD005143.
- Kruijt, B., J.-P. M. Witte, C. M. J. Jacobs, and T. Kroon (2008), Effects of rising atmospheric CO₂ on evapotranspiration and soil moisture: A practical approach for the Netherlands, *J. Hydrol.*, 349, 257–267, doi:10.1016/j.jhydrol.2007.10.052.
- Lenton, T. M., H. Held, E. Kriegler, J. W. Hall, W. Lucht, S. Rahmstorf, and J. H. Schellnhuber (2008), Tipping elements in the Earth's climate system, *Proc. Natl. Acad. Sci. U. S. A.*, 105(6), 1786–1793, doi:10.1073/pnas.0705414105.
- Loáiciga, H. A., D. R. Maidment, and J. B. Valdes (2000), Climate-change impacts in a regional karst aquifer, Texas, USA, *J. Hydrol.*, 227, 173–194, doi:10.1016/S0022-1694(99)00179-1.
- Loukas, A., L. Vasilades, and N. R. Dalezios (2002), Climatic impacts on the runoff generation processes in British Columbia, Canada, *Hydrol. Earth Syst. Sci.*, 6(2), 211–227.
- Makkink, G. F. (1957), Examination of the Penman formula (in Spanish), *Neth. J. Agric. Sci.*, 5, 290–305.
- Meehl, G. A., et al. (2007), Global climate projections, in *Climate Change 2007: The Physical Science Basis: Contribution of Working Group I to the Fourth Assessment Report of the IPCC*, edited by S. Solomon et al., 100 pp., Cambridge Univ. Press, New York.
- Mertz, E. L. (1924), Overview of the late and postglacial changes in elevation in Denmark (in Danish), *Rep. 2/41*, Geol. Surv. of Denmark and Greenland, Copenhagen.
- Mikkelsen, M. L. (2008), Flooding risks in a future climate, M. S. thesis, Inst. of Geogr. and Geol., Univ. of Copenhagen, Copenhagen.
- Mossin, L., and U. L. Ladekarl (2004), Simple water balance modeling with few data—calibration and evaluation: Investigations from a Danish Sitka spruce stand with a high interception loss, *Nord. Hydrol.*, 35(2), 139–151.
- Nash, J. E., and J. V. Sutcliffe (1970), Riverflow forecasting through conceptual models: Part 1. A discussion of principles, *J. Hydrol.*, 10, 282–290, doi:10.1016/0022-1694(70)90255-6.
- Notter, B., L. MacMillan, D. Viviroli, R. Weingartner, and H. P. Liniger (2007), Impacts of environmental change on water resources in the Mt. Kenya region, *J. Hydrol.*, 343, 266–278, doi:10.1016/j.jhydrol.2007.06.022.
- Olesen, J. E. (2005), Climate change and CO₂ effects on productivity of Danish agricultural systems, *J. Crop Impr.*, 13(1–2), 257–274, doi:10.1300/J411v13n01_12.
- Ovesen, N. B., H. L. Iversen, S. E. Larsen, D.-I. Müller-Wohlfeil, L. M. Svendsen, A. S. Blicher, and P. M. Jensen (2000), Discharge patterns in Danish streams (in Danish), *Sci. Rep.* 340, 236 pp., Natl. Environ. Res. Inst., Denmark.
- Pfister, L., J. Kwadijk, A. Musy, A. Bronstert, and L. Hoffmann (2004), Climate change, land use change and runoff prediction in the Rhine-Meuse basins, *River Res. Appl.*, 20(3), 229–241, doi:10.1002/rra.775.
- Poeter, E. P., and M. C. Hill (1998), Documentation of UCODE: A computer code for universal inverse modeling, *Water Res. Invest. Rep.* 98–4080, U. S. Geol. Surv., Denver.
- Quilbe, R., A. N. Rousseau, J. S. Moquet, S. Savary, S. Ricard, and M. S. Garbouj (2008), Hydrological responses of a watershed to historical land use evolution and future land use scenarios under climate change conditions, *Hydrol. Earth Syst. Sci.*, 12(1), 101–110.
- Refsgaard, J. C., and B. Storm (1995), MIKE SHE, in *Computer Models of Watershed Hydrology*, edited by V. P. Singh, pp. 809–846, Water Res. Publ., Highlands Ranch, Colo.
- Scharling, M. (1999), Climate grid—Denmark. Precipitation, temperature and potential evapotranspiration 20 × 20 and 40 × 40 km (in Danish), *Tech. Rep.* 99–12, 48 pp., Dan. Meteorol. Inst., Copenhagen.
- Scibek, J., and D. M. Allen (2006a), Comparing modeled responses of two high-permeability, unconfined aquifers to predicted climate change, *Global Planet. Change*, 50(1–2), 50–62, doi:10.1016/j.gloplacha.2005.10.002.
- Scibek, J., and D. M. Allen (2006b), Modeled impacts of predicted climate change on recharge and groundwater levels, *Water Resour. Res.*, 42, W11405, doi:10.1029/2005WR004742.
- Scibek, J., D. M. Allen, A. J. Cannon, and P. H. Whitfield (2007), Groundwater-surface water interaction under scenarios of climate change using a high-resolution transient groundwater model, *J. Hydrol.*, 333, 165–181, doi:10.1016/j.jhydrol.2006.08.005.
- Sonnenborg, T. O., B. S. B. Christensen, P. Nygaard, H. J. Henriksen, and J. C. Refsgaard (2003), Transient modeling of regional groundwater flow using parameter estimates from steady-state automatic calibration, *J. Hydrol.*, 273, 188–204, doi:10.1016/S0022-1694(02)00389-X.
- Thodsen, H. (2007), The influence of climate change on stream flow in Danish rivers, *J. Hydrol.*, 333, 226–238, doi:10.1016/j.jhydrol.2006.08.012.
- Thodsen, H., B. Hasholt, and J. H. Kjærsgaard (2008), The influence of climate change on suspended sediment transport in Danish rivers, *Hydrol. Processes*, 22(6), 764–774, doi:10.1002/hyp.6652.
- van der Salm, C., L. Rosenqvist, L. Vesterdal, K. Hansen, H. Denier van der Gon, A. Bleeker, R. Wieggers, and A. van den Toorn (2006), Interception and water recharge following afforestation: Experiences from oak and Norway spruces chronosequences in Denmark, in *Environmental Effects of Afforestation in North-Western Europe*, edited by G. W. Heil et al., chap. 3, pp. 53–77, Springer, Dordrecht, Netherlands.
- Vanrheenen, N. T., A. W. Wood, R. N. Palmer, and D. P. Lettenmaier (2004), Potential implications of PCM climate change scenarios for Sacramento-San Joaquin River Basin hydrology and water resources, *Clim. Change*, 62, 257–281, doi:10.1023/B:CLIM.0000013686.97342.55.
- van Roosmalen, L., B. S. B. Christensen, and T. O. Sonnenborg (2007), Regional differences in climate change impacts on groundwater and stream discharge in Denmark, *Vadose Zone J.*, 6, 554–571, doi:10.2136/vzj2006.0093.
- Varanou, E., E. Gkouvtasou, E. Baltas, and M. Mimikou (2002), Quantity and quality integrated catchment modeling under climate change with use of soil and water assessment tool model, *J. Hydrol. Eng.*, 7(3), 228–244, doi:10.1061/(ASCE)1084-0699(2002)7:3(228).
- Woldeamlak, S. T., O. Batelaan, and F. De Smedt (2007), Effects of climate change on the groundwater system of the Grote Nete catchment, Belgium, *Hydrogeol. J.*, 15(5), 891–901, doi:10.1007/s10040-006-0145-x.
- Yan, J., and K. R. Smith (1994), Simulation of integrated surface water and ground water systems: Model formulation, *Water Resour. Bull.*, 30(5), 879–890.

K. H. Jensen and L. van Roosmalen, Department of Geography and Geology, University of Copenhagen, DK-1165 Copenhagen, Denmark. (lvr@geol.ku.dk)

T. O. Sonnenborg, Geological Survey of Denmark and Greenland, Oester Voldgade 10, DK-1350 Copenhagen, Denmark.